

Available at: [http://www.ictp.it/~pub\\_off](http://www.ictp.it/~pub_off)

IC/2004/82

United Nations Educational Scientific and Cultural Organization  
and  
International Atomic Energy Agency  
THE ABDUS SALAM INTERNATIONAL CENTRE FOR THEORETICAL PHYSICS

**COULOMB EFFECTS IN RELATIVISTIC  
LASER-ASSISTED MOTT SCATTERING**

J.M. Ngoko Djiokap, M.G. Kwato Njock<sup>1</sup>

*Center for Atomic Molecular Physics and Quantum Optics, Faculty of Sciences,  
University of Douala, P.O. Box 8580, Douala, Cameroon*

*and*

*The Abdus Salam International Centre for Theoretical Physics, Trieste, Italy*

*and*

H.M. Tetchou Nganso

*Center for Atomic Molecular Physics and Quantum Optics, Faculty of Sciences,  
University of Douala, P.O. Box 8580, Douala, Cameroon.*

MIRAMARE – TRIESTE

September 2004

---

<sup>1</sup>Regular Associate of ICTP.

Corresponding author. [mkwato@yahoo.com](mailto:mkwato@yahoo.com), [mkwato\\_n@ictp.it](mailto:mkwato_n@ictp.it)

## Abstract

We reconsider the influence of the Coulomb interaction on the process of relativistic Mott scattering in a powerful electromagnetic plane wave for which the ponderomotive energy is of the order of the magnitude of the electron's rest mass. Coulomb effects of the bare nucleus on the laser-dressed electron are treated more completely than in the previous work of Li *et al.* [*J. Phys. B: At. Mol. Opt. Phys.* **37** (2004) 653]. To this end we use Coulomb-Dirac-Volkov functions to describe the initial and the final states of the electron. First-order Born differential cross sections of induced and inverse bremsstrahlung are obtained for circularly and linearly polarized laser light. Numerical calculations are carried out from both polarizations, for various nucleus charge values, three angular configurations and an incident energy in the MeV range. It is found that for parameters used in the present work, incorporating Coulomb effects of the target nucleus either in the initial state or in the final state yields cross sections which are quite similar whatever the scattering geometry and polarization considered. When Coulomb distortions are included in both states, the cross sections are strongly modified with the increase of  $Z$ , as compared to the outcome of the prior form of the T-matrix treatment.

# 1 Introduction

In recent years, impressive progress in the construction of increasingly powerful laser sources has led to the availability of beams of ultra high intensities, namely  $10^{18} \text{ W cm}^{-2}$  and above [1, 2, 3, 4]. With such beams giving rise to novel effects, it therefore has become of interest to investigate relativistic modifications of several elementary scattering processes which are of significance in many branches of physics, if they take place in a strong laser field. Among other phenomena, laser-induced Compton scattering [5, 6, 7, 8, 9], generation of high harmonics [10], laser-assisted electron scattering by a Coulomb Yukawa-type [11, 12, 13] and Coulomb potentials [14, 15] have been intensively studied. A reinvestigation of the latter process, namely the Mott scattering, focus of the present work, has been made recently by Szymanowski *et al.* [16] and Li *et al.* [17] in a circularly and linearly polarized laser field of medium and relativistic intensities. They derived analytical expressions for the spin-unpolarized cross sections under the consideration of standard Dirac-Volkov (DV) wave functions [18, 19, 20] describing the electron embedded in the joint influence of Coulomb and a vector potential. However, since the Coulomb potential is of infinitely long range, the ingoing and outgoing laser-dressed electron can never be decoupled from this field even for  $r \rightarrow \infty$ . In other words, it feels the nuclear Coulomb potential in both the entry and exit channels. Thus, the above mentioned Dirac-Volkov-based initial and final states of the electron simultaneously exposed to the laser and Coulomb field of the target nucleus, should be modified by the introduction of suitable corrections that take into account Coulomb effects.

In nonrelativistic strong laser physics, such approximative wave functions presenting a reasonable interpolation for both pure Coulomb and the plane wave fields, i.e. the so-called Coulomb-Volkov wave functions (CVF), were proposed by Jain and Tzoar [21] and Cavaliere *et al.* [22] for the first time, and have been in standard use for many years in theoretical studies. To be specific, many theoretical calculations have been carried out by various workers on laser-assisted scattering [23], multiphoton ionization [24, 25, 26, 27, 28, 29], stimulated radiative recombination and X-ray generation [30], etc. As a result, it appeared that the nuclear field plays a significant role in these processes and the CVFs could provide reliable data. For example, Duchateau *et al.* introduced a new simple non-perturbative approach to laser-induced hydrogen ionization based on Coulomb-Volkov states in which the Coulomb field of the nucleus is taken into account in the initial and final atomic states, but not in the dynamics of ionization during the laser-atom interaction. Under the sudden approximation and up to laser field amplitudes comparable to the Coulomb field of the nucleus, these authors found that the energy distributions of ejected electrons predicted by the CV method are in very good agreement with exact results obtained by a full numerical treatment of the time-dependent Schrödinger equation (TDSE) using a spherical B-spline expansion of the total wave function. Further, the Coulomb-Volkov theory proved its efficacy in providing accurate predictions with reasonable computer

times in regions where the TDSE calculations become very lengthy and finally do not converge. As for the above-threshold ionization, it is noteworthy that Coulomb effects are also important to yield the proper angular distribution of electrons in the case of elliptically polarized laser light as was demonstrated by Basile *et al.* [31] and Mu [32] describing the ejected electron instead by a Gordon-Volkov solution [33, 18] by a CVF. On the other hand, Kornev and Zon [34] applied a time-dependent generalization of the Siegert theorem to test the accuracy of the CVFs.

An earlier attempt devoted to Coulomb effects in the relativistic regime was made by Liu and Kelly [35]. They improved the relativistic strong-field-approximation (SFA) calculation by Reiss [39] of the KFR theory [36, 37, 38] that neglects the final-state interaction between the photoelectrons and the residual ion potential. Using a treatment similar to CV solution for the Schrödinger equation [40, 41], they introduced approximate Sommerfeld-Maue plus Volkov states (SMV) of the Dirac equation solved nonperturbatively for the laser field and in the first-order perturbation theory for the Coulomb potential, and investigated easily many important physical parameters over a wide range of laser intensities for multiphoton ionization processes. In the medium laser intensities, it has very recently come to our attention that a preliminary description of the laser-assisted Mott scattering in a linearly polarized laser field has been done by Li *et al.* [42]. These authors used another variant of Coulomb-Dirac-Volkov functions, i.e. a Coulomb function phase-modulated by the laser in the same way as a relativistic Volkov state, to incorporate both relativistic and initial-state Coulomb-potential effects. We refer to it as the Coulomb-Dirac-Volkov approximation (CDVI). As a step to improve this treatment, we have extended it to the final state of the electron (denoted FCDV) for relativistic laser intensities with linear [42] and circular [43] polarizations, and energetic electrons.

The organization of this paper is as follows. Section 2 describes the essentials of the theory. In section 3, we carry out a numerical study and compare our results with those obtained by Attaourti *et al.* [43] and Li *et al.* [42]. Finally in section 4, we make some concluding remarks. Atomic units ( $e = \hbar = m = 1$ ,  $c = 1/\alpha$ ) are used throughout, unless otherwise stated explicitly.

## 2 Theory

We start from the second order Dirac equation for electron in an electromagnetic field, which can be found in the well-known standard QED textbook of Berestetskii, Lifshitz and Pitaevskii [44]

$$\left[ \left( p^\mu - \frac{1}{c} A^\mu \right) \left( p_\mu - \frac{1}{c} A_\mu \right) - c^2 - \frac{1}{2c} \sigma^{\mu\nu} F_{\mu\nu} \right] \psi(x) = 0, \quad (1)$$

where  $\sigma^{\mu\nu} = \frac{i}{2}[\gamma^\mu, \gamma^\nu]$ ,  $\gamma^\mu$  are Dirac matrices,  $A^\mu = (V, \vec{A})$  is the four-vector potential and  $F_{\mu\nu} = \partial_\mu A_\nu - \partial_\nu A_\mu$  is the electromagnetic field tensor. We follow the notation used in [44]. The occurrence in this equation of the product  $\sigma^{\mu\nu} F_{\mu\nu}$  is due to the spin.

When the potential  $V$  turns off, i.e.  $A^\mu = (0, \vec{A})$ , solutions of Eq.(1) for a plane wave field first

found by Volkov [18] are reviewed by Roman *et al.* in ref. [20]. The types of positive energy which are needed here have the usual form

$$\psi = \left(1 - \frac{\not{k}\not{A}}{2c(kp)}\right) \frac{u}{\sqrt{2QV}} \exp\left(-i(qx) - i \int^{(kx)} \frac{(pA)}{c(kp)} d\varphi\right), \quad (2)$$

where  $\varphi = (kx)$ ,  $\not{k}$ ,  $\not{A}$  are denoted by the Feynman slash notation,  $u$  is the bispinor for the electron which satisfies the first-order free-particle Dirac equation  $(\not{q} - c)u = 0$ , and is normalized by the condition  $\bar{u}u = 2c^2$ . The bracket notation  $(ab)$  is a short form for the four-scalar product  $a^\nu b_\nu$ . The averaged four-momentum  $q^\mu = (Q/c, \vec{q})$  has the explicit form

$$q^\mu = p^\mu - \frac{\bar{A}^2}{2c^2(kp)} k^\mu, \quad (3)$$

where  $k^\mu = (\omega/c, \vec{k})$  is the four-vector of the electromagnetic plane wave  $k^2 = 0$ , satisfying the Lorentz gauge  $(kA) = 0$ . The renormalized energy  $Q$  and momentum  $\vec{q}$  fulfill the conservation relation  $Q^2 - c^2\vec{q}^2 = m^{*2}c^4$ , which corresponds to an outshell particle of effective mass  $m^* = (1 - \bar{A}^2/c^4)^{1/2}$ .

In contrast, when the laser field turns off, solutions of Eq.(1) for Coulomb potential  $V(r) = -Z/r$  is not separable in parabolic coordinates and cannot be obtained exactly in closed form, only in an infinite series. They were constructed approximately by Furry [46], Sommerfield and Maue [48] and are presented in Refs. [44, 46]. For positive energy, they may take the following approximative forms which asymptotically comprise a plane wave and an outgoing or an ingoing spherical waves

$$\psi^{(+)} = N \frac{u}{\sqrt{2EV}} e^{-i(px)} \left(1 - \frac{ic}{2E} \vec{\alpha} \cdot \vec{\nabla}\right)_1 F_1(i\eta, 1, i(pr - \vec{p} \cdot \vec{r})), \quad (4)$$

$$\psi^{(-)} = N^* \frac{u}{\sqrt{2EV}} e^{-i(px)} \left(1 - \frac{ic}{2E} \vec{\alpha} \cdot \vec{\nabla}\right)_1 F_1(-i\eta, 1, -i(pr + \vec{p} \cdot \vec{r})), \quad (5)$$

where

$$N = e^{\pi\eta/2} \Gamma(1 - i\eta), \quad \eta = zE/p, \quad z = \alpha Z, \quad \alpha = 1/c, \quad c = 137. \quad (6)$$

$\vec{p}$  is the electron momentum at asymptotically large distances, and  ${}_1F_1$  is the confluent hypergeometric function. These wave functions are normalized in such a way that, the plane wave in its asymptotic limit, corresponds to one particle in the volume  $V$ .

For an electron in the fields of both an attractive Coulomb centre and a laser radiation, no exact solution is available in this case. Comparing Eqs.(3)-(5), Li *et al.* [42] simply took the initial state to be an interpolating wave function given by

$$\begin{aligned} \psi_i^{(+)} &= N_i {}_1F_1(i\eta_i, 1, i(q_i r - \vec{q}_i \cdot \vec{r})) \left(1 - \frac{\not{k}\not{A}}{2c(kp_i)}\right) \frac{u_i}{\sqrt{2Q_i V}} \\ &\times \exp\left(-i(q_i x) - i \int^{(kx)} \frac{(p_i A)}{c(kp_i)} d\varphi\right), \end{aligned} \quad (7)$$

with  $N_i = e^{\pi\eta_i/2} \Gamma(1 - i\eta_i)$ ,  $\eta_i = zQ_i/q_i$ . It is worth underlining that, unlike the SMV approximate solution, the laser-field properties determines the behavior of the CDV functions trough the frequency-dependence of the four-quasimomentum  $q$  which enters the normalization factor and the argument of the  ${}_1F_1$  function. One easily verifies that Eq.(7) transforms into Eq.(4) at  $\vec{A} = 0$  and into Eq.(2) at  $Z = 0$ . It is the purpose of the present work to extend this approximation to the final ingoing wave function, namely that

$$\begin{aligned} \psi_f^{(-)} &= N_f {}_1F_1(-i\eta_f, 1, -i(q_f r + \vec{q}_f \cdot \vec{r})) \left(1 - \frac{\hbar A}{2c(kp_f)}\right) \frac{u_f}{\sqrt{2Q_f V}} \\ &\times \exp\left(-i(q_f x) - i \int^{(kx)} \frac{(p_f A)}{c(kp_f)} d\varphi\right), \end{aligned} \quad (8)$$

with  $N_f = e^{\pi\eta_f/2} \Gamma(1 - i\eta_f)$ ,  $\eta_f = zQ_f/q_f$ . The indices  $i$  and  $f$  label the initial and final states.

For considering Mott scattering in a powerful laser field in the first-order Born approximation, we have to evaluate the T-matrix element

$$T_{fi} = -i \int d^4x \bar{\psi}_f^{(-)}(x) \not{A} \psi_i^{(+)}(x), \quad (9)$$

where  $a^\mu = (-Z/r, 0, 0, 0)$  is the central Coulomb field. For our purpose, we consider the cases of circularly [16] and linearly [42] polarized laser radiation given respectively by the potential vectors

$$A = A_x \cos(\varphi) + A_y \sin(\varphi), \quad A_x = (0, |\vec{A}|, 0, 0), \quad A_y = (0, 0, |\vec{A}|, 0), \quad (10)$$

and

$$A = A_z \cos(\varphi), \quad A_z = (0, 0, 0, |\vec{A}|). \quad (11)$$

Substituting Eqs.(7) and (8) into Eq. (9), we decompose this matrix element into its Fourier components in space and time. The time integral is readily performed to extract the energy-conservation relation  $Q_f = Q_i + n\omega$  which can be presented in terms of quantities considered outside the laser beam

$$E_f = E_i - \frac{\vec{A}^2}{2c^2} \left[ \frac{1}{(kp_f)} - \frac{1}{(kp_i)} \right] + n\omega, \quad (12)$$

where  $E_f = T_f + c^2$  and  $E_i = T_i + c^2$  are the relativistic energies of the scattered and ingoing electron respectively. In most experiments, the transition rates are actually measured with unpolarized initial states and without regard to the spin orientation of the scattered electrons. Then using the usual trace technique for  $\gamma$  matrices, summing and averaging over polarizations of the electron in the final and in the initial states, one gets the following expressions for differential cross-sections

$$\frac{d\sigma}{d\Omega_f} = \sum_{n=-\infty}^{\infty} \frac{d\sigma_n}{d\Omega_f}, \quad \frac{d\sigma_n}{d\Omega_f} = |I_n|^2 \frac{d\sigma_n^{(0)}}{d\Omega_f}, \quad (13)$$

where

$$I_n = \int d^3\vec{r} \frac{e^{i\vec{q}\cdot\vec{r}}}{r} {}_1F_1(i\eta_i, 1, i(q_i r - \vec{q}_i \cdot \vec{r})) {}_1F_1(i\eta_f, 1, i(q_f r + \vec{q}_f \cdot \vec{r})), \quad (14)$$

and

$$\frac{d\sigma_n^{(0)}}{d\Omega_f} = \frac{2Z^2}{c^2} \frac{q_f}{q_i} \frac{M_n}{q^4}, \quad \vec{q} = \vec{q}_i - \vec{q}_f + n\vec{k}, \quad (15)$$

are respectively the factor in which Coulomb modifications are reflected, and the Coulomb-uncorrected differential cross sections of the laser-assisted nonlinear scattering processes of the order  $n$ , with this latter being the number of emitted (induced bremsstrahlung) and absorbed (inverse bremsstrahlung) laser photons.  $\Omega_f$  is the scattering solid angle. The nonlinear matrix elements  $M_n$  derived in Refs. [42, 43] and given below to make this article self-contained.

When the field has circular polarization,  $M_n$  has the explicit form

$$M_n = U_1 J_n^2(\zeta) + U_2 (J_{n+1}^2(\zeta) + J_{n-1}^2(\zeta)) + U_3 (J_{n+1}(\zeta) J_{n-1}(\zeta)) \\ + U_4 J_n(\zeta) (J_{n+1}(\zeta) + J_{n-1}(\zeta)), \quad (16)$$

$J_n(\zeta)$  is the ordinary Bessel function. Here, we have introduced the abbreviations

$$\zeta = \sqrt{\zeta_x^2 + \zeta_y^2}, \quad \zeta_x = \frac{(p_i A_x)}{c(kp_i)} - \frac{(p_f A_x)}{c(kp_f)}, \quad \zeta_y = \frac{(p_i A_y)}{c(kp_i)} - \frac{(p_f A_y)}{c(kp_f)}. \quad (17)$$

The coefficients  $U_1, U_2, U_3$  and  $U_4$  are found to be

$$U_1 = ((q_f q_i) - c^2) \left( \frac{A^2 \omega^2}{c^4 (kq_f)(kq_i)} - 1 \right) + \frac{2Q_i Q_f}{c^2} - \frac{A^2}{2c^2} \left( \frac{(kq_f)}{(kq_i)} + \frac{(kq_i)}{(kq_f)} \right) \\ + \frac{(A^2 \omega)^2}{c^6 (kq_f)(kq_i)} + \frac{A^2 \omega}{c^4} (Q_f - Q_i) \left( \frac{1}{(kq_i)} - \frac{1}{(kq_f)} \right), \quad (18)$$

$$U_2 = -\frac{(A^2 \omega)^2}{2c^6 (kq_f)(kq_i)} + \frac{\omega^2}{2c^4} \left( \frac{(A_x q_f)(A_x q_i)}{(kq_f)(kq_i)} + \frac{(A_y q_f)(A_y q_i)}{(kq_f)(kq_i)} \right) - \frac{A^2}{2c^2} \\ + \frac{A^2}{4c^2} \left( \frac{(kq_f)}{(kq_i)} + \frac{(kq_i)}{(kq_f)} \right) - \frac{A^2 \omega^2}{2c^4 (kq_f)(kq_i)} ((q_f q_i) - c^2) \\ + \frac{A^2 \omega}{2c^4} (Q_f - Q_i) \left( \frac{1}{(kq_f)} - \frac{1}{(kq_i)} \right), \quad (19)$$

$$U_3 = \frac{\omega^2}{c^4 (kq_f)(kq_i)} [\cos(2\phi_0) \{ (A_x q_f)(A_x q_i) - (A_y q_f)(A_y q_i) \} \\ + \sin(2\phi_0) \{ (A_x q_f)(A_y q_i) + (A_x q_i)(A_y q_f) \}], \quad (20)$$

$$U_4 = \frac{1}{2c} \left\{ (\tilde{A}q_i) + (\tilde{A}q_f) - \frac{(kq_f)}{(kq_i)} (\tilde{A}q_i) - \frac{(kq_i)}{(kq_f)} (\tilde{A}q_f) \right\} \\ + \frac{\omega}{c^3} \left( \frac{Q_i (\tilde{A}q_f)}{(kq_f)} + \frac{Q_f (\tilde{A}q_i)}{(kq_i)} \right), \quad (21)$$

where

$$\tilde{A} = A_x \cos(\phi_0) + A_y \sin(\phi_0), \quad \cos(\phi_0) = \frac{\zeta_x}{\zeta}, \quad \sin(\phi_0) = \frac{\zeta_y}{\zeta}, \quad \bar{A}^2 = -|\vec{A}|^2. \quad (22)$$

It is worth noting that Attaourti *et al.* in their comment [43] point out the differences between Eqs.(16)-(22) and the corresponding formulas presented in Ref. [16]. They claim that their result is the correct relativistic generalization of the Bunkin and Fedorov treatment [47] that is valid for an arbitrary geometry. Comparison of their numerical calculations with those of Szymanowski *et al.* shows qualitative and quantitative difference particularly for initial electron kinetic energies and electric field strength in the relativistic regime of interest in this paper. The use of the foregoing equations here stems from that point.

In the case of linear polarization, the matrix element reads

$$\begin{aligned} M_n = & c^2[\Delta_0^2 + 4(\Delta_1\Delta_2 - \Delta_0\Delta_3)A^2k_0^2] + \Delta_0^2(2p_{i0}p_{f0} - \vec{p}_i \cdot \vec{p}_f) + \Delta_1^2\{2A^2[(kp_i)(kp_f) \\ & - 2k_0p_{f0}(kp_i)]\} + \Delta_2^2\{2A^2[(kp_i)(kp_f) - 2k_0p_{i0}(kp_f)]\} + \Delta_3^2[8A^4k_0^2(kp_i)(kp_f)] \\ & + 2\Delta_0\Delta_1[2k_0p_{f0}(Ap_i) + (kp_i)(Ap_f) - (kp_f)(Ap_i)] + 2\Delta_0\Delta_2[2k_0p_{i0}(Ap_f) \\ & + (kp_f)(Ap_i) - (kp_i)(Ap_f)] + 2\Delta_0\Delta_3\{2A^2k_0[k_0(p_i p_f) - p_{i0}(kp_f) - p_{f0}(kp_i)]\} \\ & + 2\Delta_1\Delta_2\{4k_0^2(Ap_i)(Ap_f) + 2A^2[k_0p_{i0}(kp_f) + k_0p_{f0}(kp_i) - k_0^2(p_i p_f) \\ & - (kp_i)(kp_f)]\} + 2\Delta_1\Delta_3[-4A^2k_0^2(kp_i)(Ap_f)] + 2\Delta_2\Delta_3[-4A^2k_0^2(kp_f)(Ap_i)], \end{aligned} \quad (23)$$

where

$$\xi = \frac{(p_f A_z)}{c(kp_f)} - \frac{(p_i A_z)}{c(kp_i)}, \quad \Delta_0 = J_n(\xi), \quad \Delta_1 = -\frac{nJ_n(\xi)}{2c(kp_i)\xi}, \quad (24)$$

$$\Delta_2 = -\frac{nJ_n(\xi)}{2c(kp_f)\xi}, \quad \Delta_3 = \frac{J_{n-2}(\xi) + 2J_n(\xi) + J_{n+2}(\xi)}{16c^2(kp_i)(kp_f)}. \quad (25)$$

Note that we have  $\bar{A}^2 = -|\vec{A}|^2/2$  in this case.

Turning finally to the Coulomb factor  $I_n$  in Eq.(13) and following the procedure presented in Ref [45], we obtain in closed form

$$I_n = N_i N_f^* \left(\frac{D_1}{q^2}\right)^{-in_f} \left(\frac{D_2}{q^2}\right)^{-in_i} {}_2F_1(in_i, in_f; 1; \rho), \quad (26)$$

where

$$D_1 = (\vec{q}_i + n\vec{k})^2 - q_f^2, \quad D_2 = (\vec{q}_f - n\vec{k})^2 - q_i^2, \quad (27)$$

$$\rho = 2 \frac{q^2 [q_i q_f + \vec{q}_i \cdot \vec{q}_f - 2(\vec{q} \cdot \vec{q}_i)(\vec{q} \cdot \vec{q}_f)]}{(q^2 - \vec{q} \cdot \vec{q}_i)(q^2 + \vec{q} \cdot \vec{q}_f)}, \quad (28)$$

and  ${}_2F_1$  is the hypergeometric function [49].



When examining of Eq.(26), we note two limiting cases of interest. Firstly, if the Coulomb field of the residual ion is taken into account only in the initial state, i.e.  $\eta_f = 0$ , Eq. (26) becomes

$$I_n = e^{\pi\eta_i/2} \Gamma(1 - i\eta_i) \left( \frac{D_2}{q^2} \right)^{-i\eta_i}, \quad (29)$$

which is identical with Eq.(9) of [42] by Li *et al.* in which  $\vec{q}_i$  and  $\vec{q}_f$  should be replaced by  $-\vec{q}_i$  and  $-\vec{q}_f$  respectively. Secondly, including the Coulomb distortion in the final state, i.e.  $\eta_i = 0$ , leads to

$$I_n = e^{\pi\eta_f/2} \Gamma(1 + i\eta_f) \left( \frac{D_1}{q^2} \right)^{-i\eta_f}. \quad (30)$$

We have used Eqs.(29) and (30) to evaluate the effects of the initial- (CDVI prior form) and final-state (CDVF post form) Coulomb potential respectively. It should be noticed that these prior and post Coulomb factors are not identical which means that a difference between both forms may occur in the relativistic regime.

### 3 Numerical examples

In this section, the results of applications of the foregoing equations are presented by numerically evaluating the differential cross-sections for several values of the charge of the nucleus, namely  $Z = 1, 5, 10, 15, 20, 25, 30, 35, 40$ . We have chosen the angular frequency  $\omega = 0.043$  *a.u.* of a Nd:YAG laser, the electrical field  $E = 5.89$  *a.u.* of relativistic strength and the kinetic energy of ingoing electron  $T_i = 4c^2$  in the MeV range, for all numerical evaluations. We assume that the origin of the coordinate system coincides with the target which is supposed to be an infinitely massive nucleus.  $\theta$  and  $\phi$  denote the usual polar and azimuthal angles in spherical coordinates. In order to assess the influence of the polarization on Coulomb effects in this regime, we have considered the two cases of circularly and linearly polarized laser field described in Refs. [17, 42]. In the scattering geometry of the first case, the  $z$ -axis is set along the field wave vector  $\vec{k}$  (meaning that  $\theta_\gamma = \phi_\gamma = 0$ ), the  $x$ -axis along the direction of the incident electron ( $\theta_i = \pi/2, \phi_i = 0$ ), the momentum of the outgoing electron  $\vec{p}_f$  is supposed to be either in the  $yz$ -plane ( $\phi_f = \pi/2, 3\pi/2$ , scattering geometry denoted SG1) or in the  $xy$ -plane ( $\theta_f = \pi/2$ , SG2). As for the second case, SG3 is defined by  $\theta_\gamma = \phi_\gamma = \pi/2, \theta_i = \phi_i = 0$  and  $\phi_f = 0, \pi$ .

First of all, we have not reported the CDVF results because they are practically identical to those of CDVI whatever the parameters  $T_i$  and  $Z$  used in the circular and linear polarizations laser field in the figures presented below. In other words, the difference between both forms is negligible. This has already been pointed out by Li *et al.* [42] for the medium field laser intensity considered in their calculation.

Figures 1 and 2 show the differential cross sections summed over  $\pm 100$  multiphoton processes around the elastic peak as a function of the angle  $\theta_f$  for the scattering geometry SG1 as given by

Eqs. (13), (15), (16). Included in figure 2 are the results for FCDV (solid line), CDVI (dashed line) and the DV (dash-dotted line). Qualitatively, they exhibit almost the same shape and maxima occur for  $\theta_f = 0, \pm 180^\circ$ . From a physical point of view, this shape is comprehensible because according to the SG1 geometry, scattering at these angles requires a close encounter with the target nucleus. Quantitatively, The difference between CDVI and DV is not so striking for  $Z = 1$ . As  $Z$  increases to 40, the FCDV summed differential cross sections are greatly enhanced steadily by about two orders. In contrast, the CDVI cross sections do not show such a behavior as compared to the DV ones. This clearly indicates the strong coupling of the electron with the nucleus in the initial and final states.

In figures 3 and 4, an analogous comparison is made for the scattering geometry SG3 of linear polarization laser field. The values of parameters used here are the same as in figures 1 and 2 respectively. At small scattering angles FCDV, CDVI and DV curves merge together since the Coulomb distortion in the electron initial and final states is less prominent at large impact parameters. With the increase of  $Z$  to 40, FCDV and CDVI curves varying tendencies with respect to DV are more or less the same as in circular case.

For getting a better idea on the incorporation of the Coulomb field effects of the nucleus in FCDV and CDVI approaches, let

$$\Delta\sigma = \frac{|d\sigma_a/d\Omega_f - d\sigma_b/d\Omega_f|}{d\sigma_a/d\Omega_f + d\sigma_b/d\Omega_f} \quad (31)$$

be a measure of the difference between  $d\sigma_a/d\Omega_f$  and  $d\sigma_b/d\Omega_f$  data. This normalized difference which can have the values  $0 \leq \Delta\sigma \leq 1$  was introduced by Panek *et al.* [13]. For comparative purposes, we have the considered scattering geometries SG2 and SG3 for  $\theta_f = \pi/2$ . In addition, the azimuthal angle is  $\pi/2$  and 0 in the former and the latter respectively. The results obtained for FCDV and CDVI with DV as reference values are depicted in figures 5 and 6. It clearly appears that the deviation between CDVI and DV is small and only gradually increases for  $Z$  approaching 40. In contrast, a significance discrepancy between FCDV and DV is recognized for  $Z$  higher than 10. The higher the charge is, the more the electron states are distorted, thus the more the cross section is modified. This has led us to evaluate in the angular distribution once more the difference  $\Delta\sigma$  between FCDV and CDVI as a function of  $Z$ . The results obtained are displayed in figures 7, 8 and 9. For the data presented, we have chosen in figure 8, i.e. for SG1 geometry,  $\theta_f = \pi/2$  and  $0 \leq \phi_f \leq 180$  the angle between the ingoing and scattered electron in the  $xy$ -plane. We observe that the deviations are particularly large for  $Z$  higher than 10 whatever the scattering geometry and the polarization of the laser field. However, the spectra are not so smooth but rather show some structures.

## 4 Conclusion

In the present work we have investigated the Mott scattering taking place in a relativistic laser intensity, when Coulomb field of the target nucleus is taken into account in the electron

initial and final states. Coulomb-corrected Dirac-Volkov wavefunctions proposed recently by Li *et al.* have been used to describe an electron moving under the joint influence of a Coulomb and a vector potential. We have considered three scattering configurations, a laser field of relativistic intensity, and a kinetic energy of the projectile in the MeV range. Cross sections for this laser-assisted process have been obtained with circularly and linearly polarized light for various nucleus charge values. The CDVI and CDVF results are identical, but both of them are about two orders of magnitude smaller than the FCDV ones. The fact that Coulomb interaction significantly enlarges the latter outcome presumably shows that the prior and post form approximations are less realistic.

## Acknowledgments

Two of us (J.M.N.D and M.G.K.N.) gratefully acknowledge the financial support from the Swedish International Development Agency (SIDA) for their visits to the Abdus Salam International Centre for Theoretical Physics (ICTP) under the Associateship Scheme. The authors are also indebted to Professor G. Denardo for warm hospitality at the Abdus Salam International Centre for Theoretical Physics where this work was executed.

## References

- [1] C. Joshi, B. Blue, C.E. Clayton, E. Dodd, C. Huang, K.A. Marsh, W.B. Morri, S. Wang, M.J. Hogan, C. O'Connell, R. Siemann, D. Watz, P. Muggly, T. Katsouleas and S. Lee *Phys. Plasmas*. **9** (2002) 1845.
- [2] V. Bagnoud and F. Salin *1.1 terawatt kilohertz femtosecond laser, invited talk*, Conference on lasers and Electro-Optics (CLEO), CTuD3, Baltimore (23-28 May 1999).
- [3] P.A. Norreys, M. Zepf, S. Monstaizis, A.P. Fewes, J. Zhang, P. Lee, M. Bakerezos, C.N. Danson, A. Dyson, P. Gibbon, P. Lonkakos, D. Neely, F.N. Walsh, J.S. Wark, A.E. Dangor *Phys. Rev. Lett.* **76** (1996) 1832.
- [4] H. Milchberg and R. Freeman *J. Opt. Soc. Am. B* **13** (1996) 51.
- [5] I.I. Gol'dman *Zh. Eksp. Teor. Fiz.* **46** (1964) 1412 [*Sov. Phys. JETP* **19** (1964) 954].
- [6] C.I. Moore, J.P. Knauer and D.D. Meyerhofer *Phys. Rev. Lett.* **74** (1995) 2439.
- [7] L. Rosenberg *Phys. Rev. A* **49** (1994) 1122.
- [8] C. Bula, K.T. McDonald, E.J. Prebys, C. Bamber, S. Boege, T. Kotseroglon, A.C. Melissinos, D.D. Meyerhofer, W. Ragg, D.L. Burke, R.C. Field, G. Horton-Smith, A.C. Odian, J.E. Spencer, D. Walz, S.C. Berridge, W.M. Bugg, K. Shmakov and A.W. Weidemann *Phys. Rev. Lett.* **76** (1996) 3116.
- [9] V.F. Hartemann and A.K. Kerman *Phys. Rev. Lett.* **76** (1996) 624.
- [10] M. Protopapas, C.H. Keitel and P.L. Knight *Rep. Prog. Phys.* **60** (2002) 389.
- [11] C. Szymanowski and A. Maquet *Opt. Express*. **2** (1998) 262.
- [12] J.Z. Kaminski and F. Ehlotzky *Phys. Rev. A* **59** (1999) 2105.
- [13] P. Panek, J.Z. Kaminski and F. Ehlotzky *Phys. Rev. A* **65** (2002) 033408.
- [14] M.M. Denisov and M.V. Fedorov *Zh. Eksp. Teor. Fiz.* **53** (1968) 1340 [*Sov. Phys. JETP* **26** (1968) 779].
- [15] S.P. Roschchupkin *Zh. Eksp. Teor. Fiz.* **106** (1994) 102 [*Sov. Phys. JETP* **79** (1994) 54]; *ibid Zh. Eksp. Teor. Fiz.* **82** (1996) 177 [*Sov. Phys. JETP* **109** (1996) 337].
- [16] C. Szymanowski, V. Véniard, R. Taieb, A. Maquet and C.H. Keitel *Phys. Rev. A* **56** (1997) 3846.
- [17] S.-M. Li, J. Berakdar, J. Chen and Z.-F. Zhou *Phys. Rev. A* **67** (2003) 063409.
- [18] D.M. Volkov *Z. Phys.* **94** (1935) 250.
- [19] J. Bergon and S. Varro *J. Phys. A: Math. Gen.* **13** (1980) 2823.
- [20] J.S. Roman, L. Roso and H.R. Reiss *J. Phys. B: At. Mol. Opt. Phys.* **33** (2000) 1869.
- [21] M. Jain and N. Tzoard *Phys. Rev. A* **18** (1978) 538.
- [22] P. Cavaliere, G. Ferrante and C. Leone *J. Phys. B: At. Mol. Opt. Phys.* **13** (1980) 4495.

- [23] S.-M. Li, Y.-G. Miao, Z-F. Zhou, J. Chen and Y.-Y. Liu *Phys. Rev. A* **58** (1998) 2615.
- [24] G. Duchateau, C. Illescas, B. Pons, E. Cornier and R. Gayet *J. Phys. B: At. Mol. Opt. Phys.* **33** (2000) L571.
- [25] G. Duchateau, E. Cornier and R. Gayet *Eur. Phys. J. D* **11** (2000) 191.
- [26] S.-M. Li, J. Chen and Z-F. Zhou *J. Phys. B: At. Mol. Opt. Phys.* **35** (2002) 557.
- [27] J.Z. Kaminski, A. Jaron and F. Ehlotzky *Phys. Rev. A* **53** (1996) 1756
- [28] H.R. Reiss and V.P. Krainov, *Phys. Rev. A* **50**, (1994) R910.
- [29] H.R. Shakeshaft and R.M. Potvilege, *Phys. Rev. A* **36**, (1987) 5478.
- [30] A. Jaron, J.Z. Kaminski and F. Ehlotzky *Phys. Rev. A* **61** (2000) 023404.
- [31] S. Basile, F. Trombetta and G. Ferrante *Phys. Rev. Lett.* **61** (1988) 2435.
- [32] X. Mu *Phys. Rev. A* **43** (1991) 5149.
- [33] W. Gordon *Z. Phys.* **40** (1926) 117.
- [34] A.S. Kornev and B.A. Zon *J. Phys. B: At. Mol. Opt. Phys.* **35** (2002) 2451.
- [35] Z.W. Liu and H.P. Kelly *Phys. Rev.* **47** (1993) 1460.
- [36] L.V. Keldysh *Zh. Eksp. Teor. Fiz.* **47** (1965) 1945 [*Sov. Phys. JETP* **20** (1965) 1307].
- [37] F. Faisal *J. Phys. B: At. Mol. Opt. Phys.* **6** (1973) L89.
- [38] H.R. Reiss *Phys. Rev. A* **22** (1980) 1786.
- [39] H.R. Reiss *J. Opt. Soc. Am. B* **7** (1990) 574.
- [40] C. Leone, R. Burlon, F. Trombetta, S. Basile and G. Ferrante *Nuovo Cimento D* **9** (1987) 609.
- [41] F. Trombetta, S. Basile and G. Ferrante *J. Opt. Soc. Am. B* **6** (1989) 554.
- [42] S.-M. Li, J. Berakdar, J. Chen and Z.-F. Zhou *J. Phys. B: At. Mol. Opt. Phys.* **37** (2004) 653.
- [43] Y. Attaourti and B. Manaut *Phys. Rev. A* **68** (2003) 067401.
- [44] V.B. Berestetskii, E.M. Lifshitz and Pitaevskii *Quantum Electrodynamics (Course of Theoretical Physics Vol 4)* 2nd edn (Pergamon Press, 1982).
- [45] L. Bess *Phys. Rev.* **77** (1950) 550.
- [46] W.H. Furry *Phys. Rev.* **46** (1934) 391.
- [47] F.V. Bunkin and M.V. Fedorov *Zh. Eksp. Teor. Fiz* **49** (1966) 1215 [*Sov. Phys. JETP* **22** (1966) 844].
- [48] A. Sommerfeld and A.W. Maue *Ann. d. Physik.* **22** (1935) 629.
- [49] M. Abramowitz and I.A. Stegun (ed) *Handbook of Mathematical Functions with formulas, graphs and mathematical tables*, (Dover Publications, 1972).

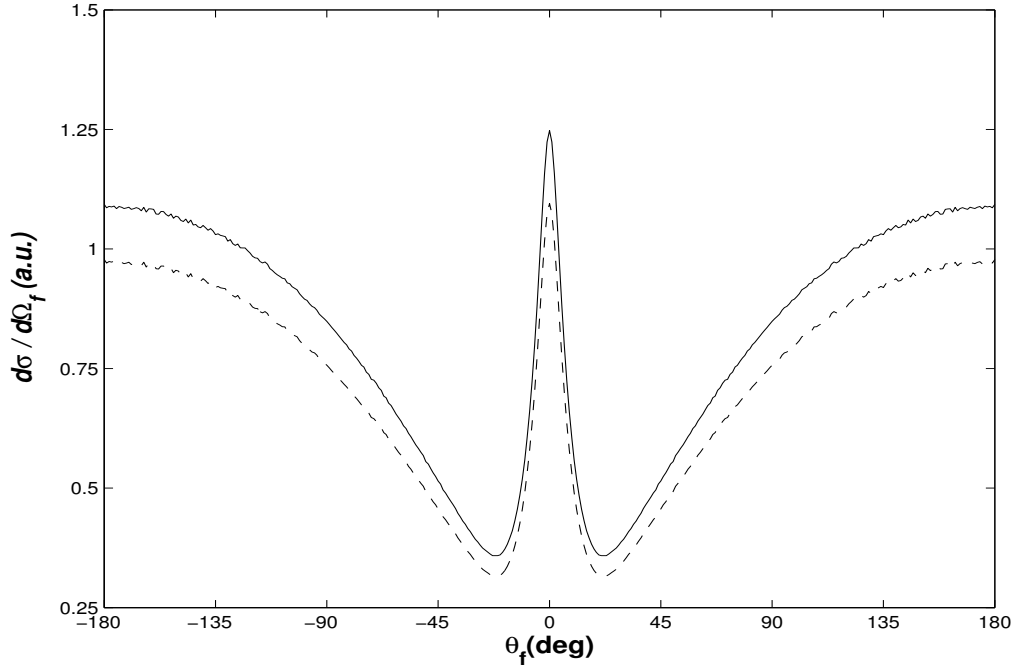


Figure 1: Plot of the summed differential cross sections in a.u. of  $\pm 100$  peaks around the elastic one versus the angle  $\theta_f$  for the scattering geometry SG1 in the case of circular polarization. The nucleus charge is  $Z = 1$ . The solid line is the FCDV result and the dashed one sketches the values obtained within CDVI.

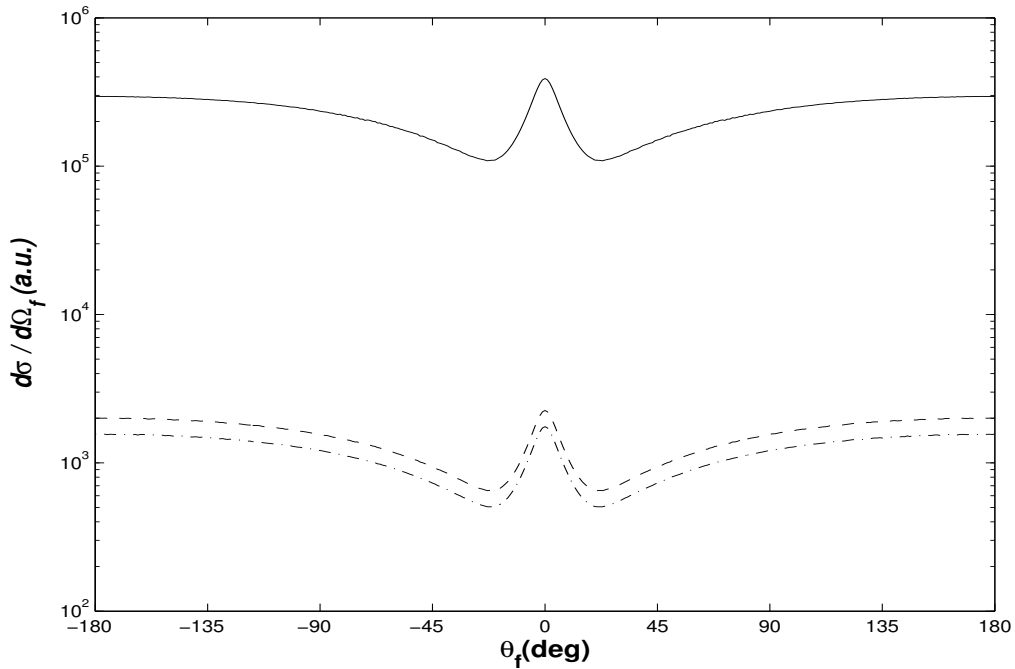


Figure 2: Plot of the summed differential cross sections in a.u. of  $\pm 100$  peaks around the elastic one versus the angle  $\theta_f$  for the scattering geometry SG1 in the case of circular polarization. The nucleus charge is  $Z=40$ . The solid line is the FCDV result, the dashed and dash-dotted lines denote values obtained within CDVI and DV.

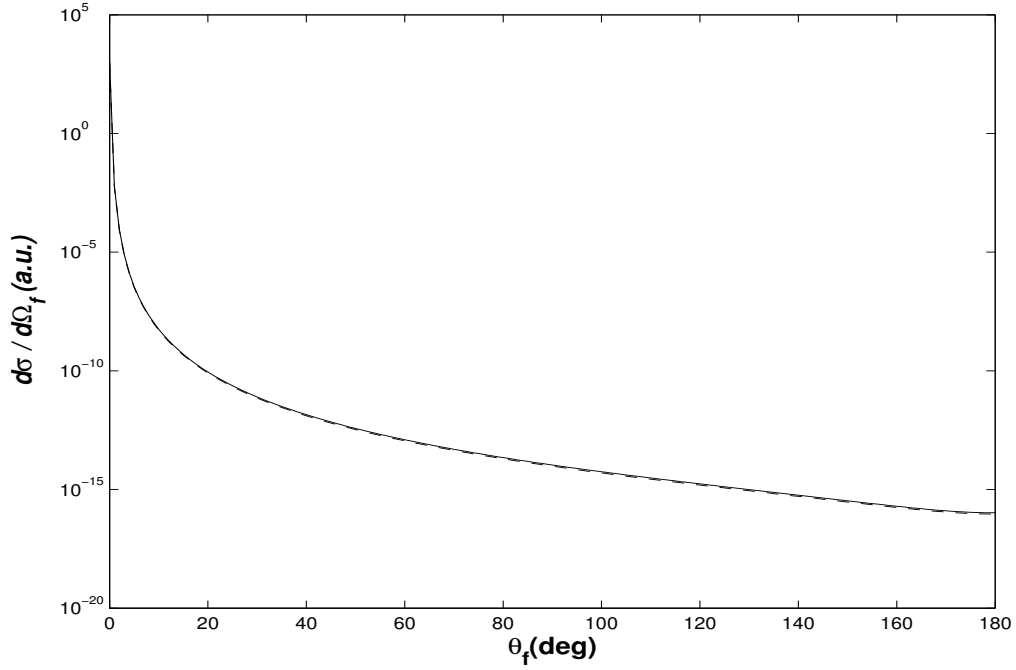


Figure 3: Plot of the summed differential cross sections in a.u. of  $\pm 100$  peaks around the elastic one versus the angle  $\theta_f$  for the scattering geometry SG3 in the case of the linear polarization. The nucleus charge is  $Z = 1$ . The solid line is the FCDV result and the dashed one sketches the values obtained within CDVI.

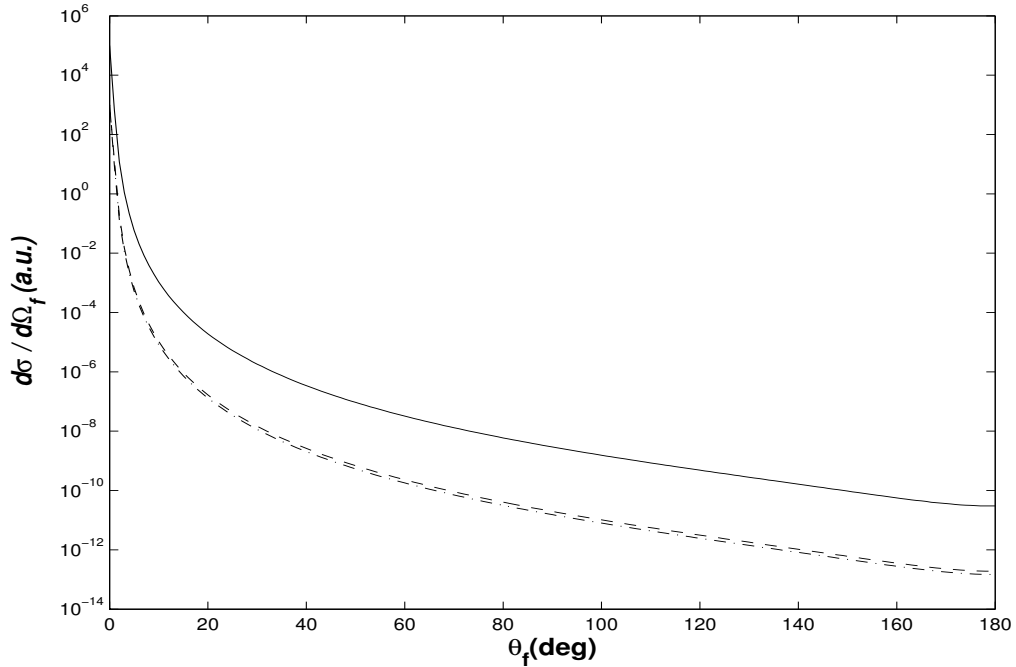


Figure 4: Plot of the summed differential cross sections in a.u. of  $\pm 100$  peaks around the elastic one versus the angle  $\theta_f$  for the scattering geometry SG3 in the case of the linear polarization. The nucleus charge is  $Z = 40$ . The solid line the FCDV result, the dashed and dash-dotted lines denote values obtained within CDVI and DV.

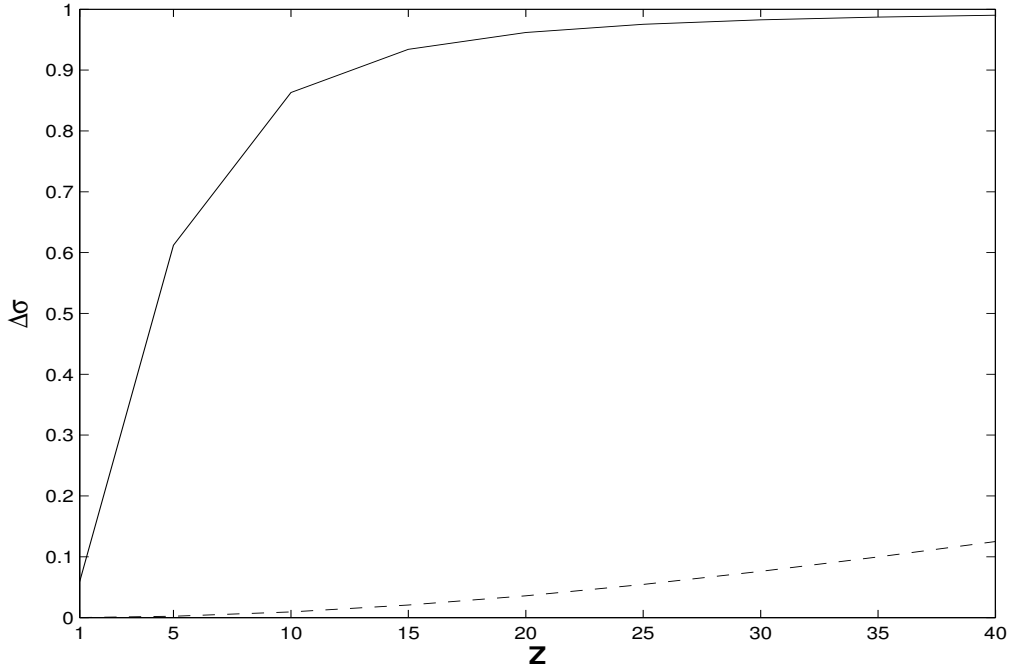


Figure 5: Normalized deviations of the FCDV (solid line) and CDVI (dashed line) cross sections from DV ones as a function of the nucleus charge for SG2 in the case of circular polarization. For comparative purpose with the linear polarization, the scattering direction is  $\theta_f = \phi_f = \pi/2$ . Curves are drawn to guide the eye.

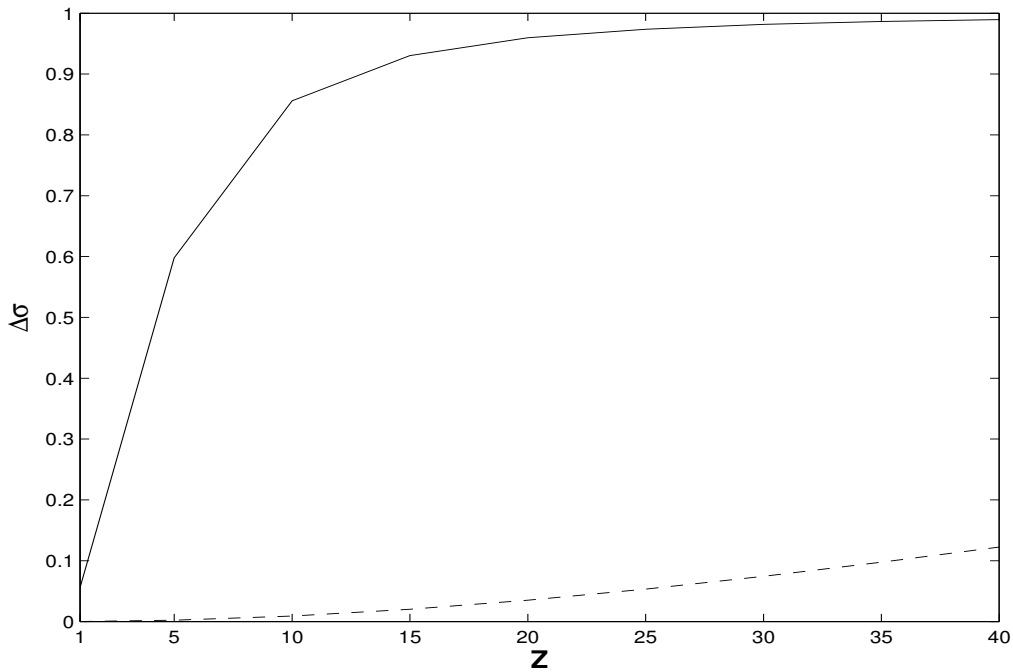


Figure 6: Normalized deviations of the FCDV (solid line) and CDVI (dashed line) cross sections from DV ones as a function of the nucleus charge for SG3 in the case of linear polarization. Curves are drawn to guide the eye.



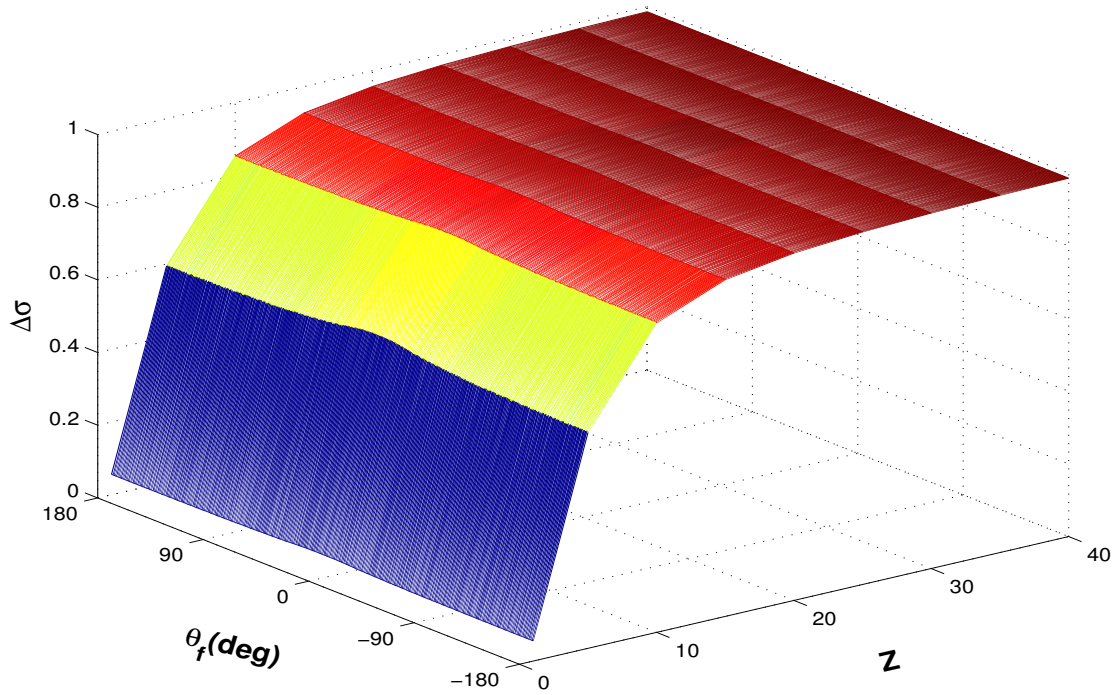


Figure 7: Normalized deviations of the FCDV cross sections from the CDVI ones versus the angle  $\theta_f$  and the nucleus charge for SG1 in the case of circular polarization.

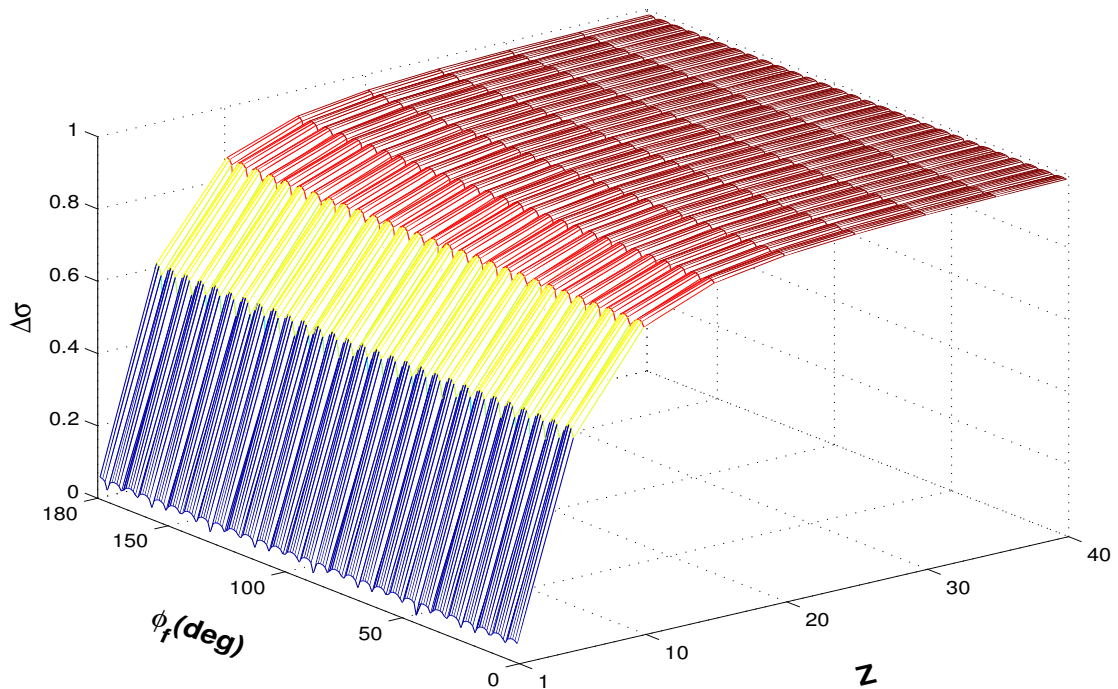


Figure 8: Normalized deviations of the FCDV cross sections from the CDVI ones versus the angle  $\phi_f$  and the nucleus charge for SG3 in the case of circular polarization.

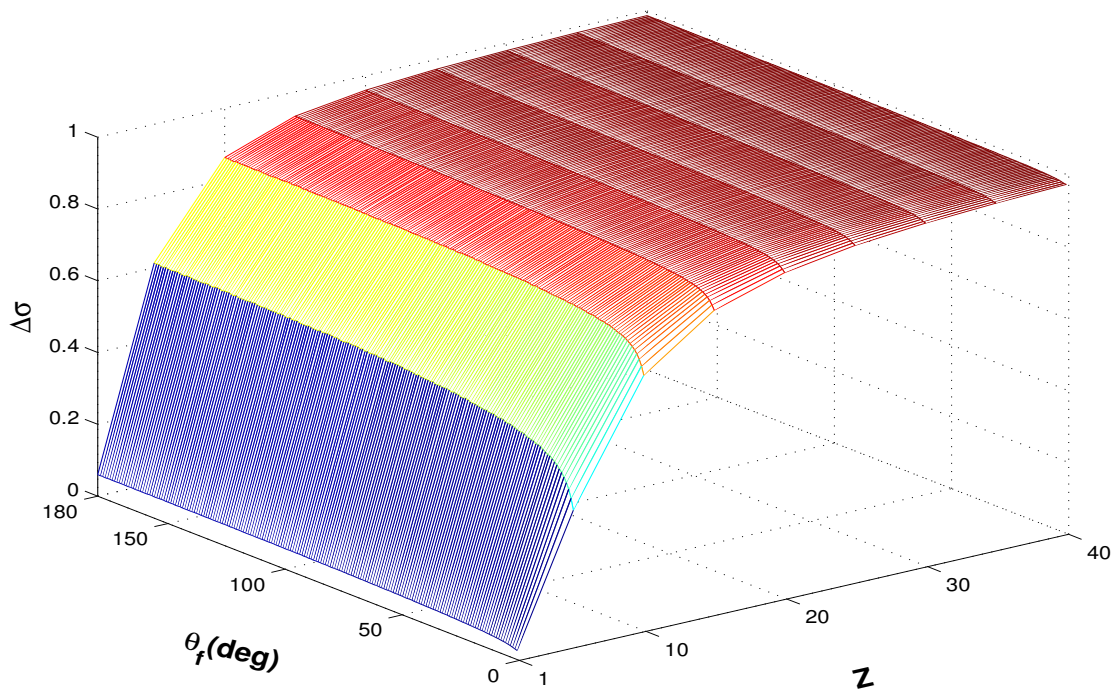


Figure 9: Normalized deviations of the FCDV cross sections from the CDVI ones versus the angle  $\theta_f$  and the nucleus charge for SG2 in the case of linear polarization.